

## Modeling pore blocking of nanofiltration and reverse osmosis membranes during NaCl removal

M. Bchiti<sup>1</sup>, M. Igouzal<sup>2\*</sup>, S. El-Ghizel<sup>1</sup>, A. El Midaoui<sup>1</sup>

<sup>1</sup> *Laboratory of Advanced Materials and Process Engineering, Department of Chemistry, Faculty of Science, Ibn Tofail University, BP1246 Kenitra, Morocco*

<sup>2</sup> *Laboratory of Electronic Systems, Information Processing, Mechanics and Energy, Department of Physics, Faculty of Science, Ibn Tofail University, BP1246 Kenitra, Morocco*

Received: December 12, 2021; Revised: May 11, 2022

Moroccan surface water and groundwater mark an increase of salt concentrations in the authorized drinking water levels. Membrane processes are a helpful technology to minimize these concentrations and to achieve high water quality in the distribution systems. However, the performance of a given membrane is found to be degraded due to membrane fouling and hence it results into a significant decline in the permeate flux. Membrane fouling is mainly associated with the deposition of solute molecules on the membrane surface. Therefore, it is necessary to interpret the fouling mechanism in order to predict the permeate flux evolution. In this paper, the permeate flux decline with time through two nanofiltration (NF) membranes (NF90, NF270) and one reverse osmosis (RO) membrane (BW30LE4040) was studied at a laboratory pilot scale using synthetic water doped with NaCl. Then, the mechanism of membrane fouling was studied through describing four pore-blocking models such as Complete Pore Blocking, Standard Pore Blocking, Intermediate Pore Blocking and Cake Formation. Parameters of these models were evaluated using a mathematical optimization procedure. The accuracy of the fitted model was judged using the statistical parameters: regression coefficient, root mean square error (RMSE), normalized root mean square error (NRMSE) and Nash-Sutcliffe efficiency (NSE). Results show that the Complete Pore Blocking Model was the best representation of pore blocking and permeate flux decline of RO and NF membranes in filtration operations.

**Keywords:** Nanofiltration, Reverse osmosis, Fouling, Permeate flux, Pore blocking model.

### INTRODUCTION

Morocco is enduring water shortage and a wide variation of rainfalls which will worsen over the next few years. The concentration of inhabitants and consequently the industrial and agricultural activities along the coastal zone have led to an increase in drinking water demand along this area. Seawater and groundwater desalination can provide a solution to this problem. Hence, many desalination plants were built using RO /NF membranes in water applications.

NF and RO are technologies being increasingly employed to enhance the quality of purified water, increase the productivity of existing plants, and design smaller, yet more effective purification processes.

Choosing the most appropriate membranes for a given water treatment project is decisive [1-4]. Membrane performances must be studied first in a pilot scale, especially for situations where process uncertainties are potentially high in terms of membranes performance and total operation cost [5-7]. Unfortunately, a barrier to a breakthrough of the technology is the increased operational cost due to fouling and membrane replacement. Simulation studies with rigorous process models are a powerful

tool to increase the understanding of the process and its decisive characteristics in order to design optimal processes and efficient operational strategies. The membrane fouling is affected by several factors, e.g., pore blocking and/or pore constriction, cake formation, solute adsorption, and concentration polarization [8-11]. Initially, foulants smaller than the pore size of membrane deposit or adsorb onto the pore walls, thereby leading to pore constriction. This induces a significant reduction in the cross-sectional area available to the filtrate flow. In contrast, larger foulants deposit or adsorb onto the pore entrances, resulting in a marked increase in the filtrate flow resistance. In either case, pore constriction and pore plugging are followed by the formation of a filter cake accumulating on the membrane surface, thus severely increasing the filtration resistance. Therefore, it is essential to elucidate the underlying mechanism controlling the membrane fouling such as pore constriction, pore plugging, and cake formation during the course of membrane filtration.

Simulation studies with rigorous process models are a powerful tool to increase the understanding of the process and its decisive characteristics in order to design optimal processes

\*To whom all correspondence should be sent:

E-mail: [mohammed.igouzal@uit.ac.ma](mailto:mohammed.igouzal@uit.ac.ma)

and efficient operational strategies.

Different models have been proposed in the literature to explain the flux decline. Prominent amongst these are the Standard Blocking Model, Intermediate Blocking Model, Cake Formation Model and Complete Blocking Model [12]. In the Standard Blocking Model, particles get accumulated inside the membrane on the pore walls and the resulting constriction of pores reduces the membrane's permeability. Intermediate Blocking Model assumes that a portion of particles seal some of the pores while the rest accumulate on the top of the deposited particles. The Complete Blocking Model is based on the premise that the particles are larger than the pore size of the membrane and this results in the particles sealing off the membrane and preventing the flow. Finally, the Cake Formation Model assumes particle accumulation on the membrane surface in a permeable cake of increasing thickness. These mechanisms have been used individually, as well as in combination to explain experimental observations [12].

Earlier works of our laboratory [13] have shown that the permeate flux decreases overtime, due to fouling, so an increase in feed water pressure is operated to ensure a constant permeate flow. Also, improvement in permeate flow rate is accompanied by an enhancement of fouling. In addition, the improved hydraulic performance of the plant occurs immediately after cleaning the fouled membranes.

On the other hand, samples of membrane and fouling were analyzed using a scanning electron microscope (SEM). Results showed that the fouling layer is mainly composed of calcium carbonate [14].

Therefore, in the present study, the permeate

flux temporal evolution through two NF membranes (NF90, NF270) and one RO membrane (BW30LE4040) is studied by analyzing various pore blocking models for NaCl removal.

The fouling process is characterized through four pore blocking models as described above. It was found that the Complete Pore Blocking Model exhibited better fit with the experimental data with a reasonably high value of the regression coefficient ( $R^2 \approx 0.95$ ).

## MATERIAL AND METHODS

### Pilot used

Experiments were performed in an NF/RO pilot plant (E 3039) supplied by TIA Company (Technologies Industrielles Appliquées, France). The pressure applied over the membrane can be varied from 5 to 70 bars with manual valves (Fig. 1). The pilot is equipped with two identical spiral-wound modules operating in series. Each module contains one element. The pressure loss is about 2 bars corresponding to 1 bar of each module. Table 1 gives the characteristics of the commercial membranes. Feed water salinity is  $2 \text{ g L}^{-1}$ . The treatment pilot is operated in semi-batch mode, i.e. the permeate is recovered, and the retentate is continuously recycled in the feed tank. This option allows continuous water treatment and approximates industrial conditions. The pressure was set for each membrane at 8 bar in order to have the same operating conditions in terms of pressure for the three studied membrane (BW30, NF90 and NF270) and the experiments were performed at  $20^\circ\text{C}$ . Samples of permeate were collected and the water parameters were determined analytically following the standard.

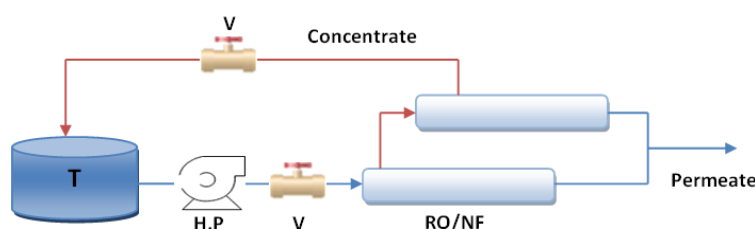


**Fig. 1.** Schematic diagram of the nanofiltration/reverse osmosis pilot plant. T: tank; H.P: High pressure pump; V: pressure regulation valve.

**Table 1.** Characteristics of the membranes

Membrane	Surface (m <sup>2</sup> )	P <sub>max</sub> (bars)	Feed pH	Max. T (°C)	Material	Manufacturer
BW30LE4040	7.6	41	2-11	45	Polyamid	Filmtec
NF90	7.6	40	3-10	45	Polyamid	Filmtec
NF270	7.6	40	3-10	45	Polyamid	Filmtec

### Mathematical model

Flux decline for a constant pressure dead-end filtration can be described by the following mathematical expression [12]:

$$\frac{d^2t}{dV^2} \left( \frac{dt}{dV} \right)^n \quad (1)$$

where  $t$  is the filtration time,  $V$  is the total filtered volume and  $n$  is an exponent that depends on the fouling model ( $n = 2$  for complete pore blockage,  $n = 1.5$  for pore constriction,  $n = 1$  for intermediate blockage and  $n = 0$  for cake formation) (Fig. 2).

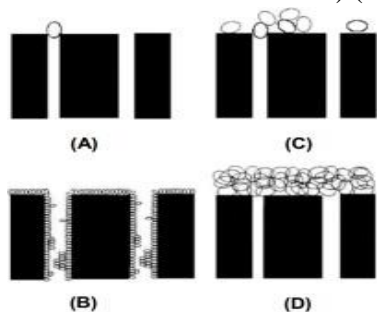


**Figure 2.** Schematic drawing of the assumed fouling mechanisms: (A) complete blocking; (B) internal pore blocking; (C) intermediate blocking; (D) cake formation [15].

For  $n=2$  (Complete Blocking Model), the size of the particles is larger than that of the membrane pore; particles deposit on the membrane surface and block the entrances of membrane pores completely with no overlapping particles.

For  $n=1.5$  (Standard Blocking Model), the internal volume of the pores decreases proportionally to the permeate volume due to deposition or adsorption of microsolute on the pore walls. Material not rejected by the pore entrance is adsorbed or trapped on the pore wall or in the membrane support, thus leading to a decrease in pore volume.

For  $n=1$  (Intermediate Pore Blocking Model), each particle arriving at the membrane settles on another particle, which had arrived previously and was already blocking some pore, or directly blocks some membrane area;

For  $n=0$  (Cake Formation Model), each particle locates on others that have already arrived and are blocking some pores and there is no room for directly obstructing any membrane area.

The permeate flux is presented as [16]:

$$J = \frac{1}{A} \frac{dV}{dt} \quad (2)$$

which can be written as:

$$\frac{dt}{dV} = \frac{1}{A \cdot J} \quad (3)$$

Taking the derivative of Eq. 3 with respect to  $t$  and substituting in Eq. 1, we obtain the governing equation of flux decline with time as follows [16]:

$$\frac{dJ}{dt} = -\alpha J^{3-n} \quad (4)$$

where  $\alpha$  is a constant and  $n$  is a general index which depends on fouling mechanism. The analytical solutions of Eq. 4 for each  $n$  value, as well as the linear forms of flux expressions are listed in Table 2, where  $J_0$  is initial flux and  $K_b$ ,  $K_s$ ,  $K_i$  and  $K_c$  are model parameters [16].

### Optimization and statistical analysis

To identify the fouling mechanism, the parameters  $K_b$ ,  $K_s$ ,  $K_i$  and  $K_c$  were estimated according to the nonlinear regression optimization procedure. The sum of the squares of the residuals between numerical predictions and experimental data was minimized [17]. Optimization runs were performed sequentially for each set  $J \times t$  by assigning ( $n = 0, 1.0, 1.5, 2.0$ ).

Additional statistical parameters were examined, as root mean square error (RMSE), normalized root mean square error (NRMSE) and Nash-Sutcliffe efficiency (NSE) coefficient. The RMSE is the distance, on average, of a data point from the fitted line. The NRMSE calculates the residual variance. The NSE is a normalized statistic that determines the relative magnitude of the residual variance (noise) compared to the measured data variance (information).

## RESULTS AND DISCUSSION

Calculated model parameters of flux decline for all membranes are summarized in Table 3.

Fig. 3 shows good fit between observed and calculated flux. However, according to statistical results in Table 3, the Complete Blocking Model was the mathematic model that best represented flux decline with time for BW30L E4040, NF270 and NF90, as  $R^2$  is above 0.95 for this model. Table 3 also shows that the cake formation model was the farthest away from the experimental data, showing that cake formation was discrete, or did not occur at all, in the membranes.

Table 4 shows the results of the statistical analysis, for the Complete Blocking Model, as described in the Material and methods section. The RMSE coefficient obtained has a small value, the NRMSE function is less than unity and the NSE coefficient is close to 1. This result demonstrates the

good performance of this model and of the optimization procedure. Also, the permeate flux decline *versus* time for the three membranes is presented in Fig. 3. According to the figure, the observed permeate flux is continually reduced due to concentration polarization and fouling phenomena.

Fig. 4 shows the cumulative permeate volume per unit membrane surface *versus* time. It indicates a continuous increase of the current flux with time that is well represented by the Complete Blocking Model.

**Table 2.** Solutions of Eq. 4 for different n values

Model	(a) Complete blocking	(b) Standard blocking	(c) Intermediate blocking	(d) Cake formation
$\frac{d^2t}{dv^2} = k \left(\frac{dt}{dv}\right)^n$	n = 2.0	n = 1,5	n = 1	n = 0
J=f(t)	$J = J_0 \exp(-K_b t)$	$J = \frac{J_0}{\left(\frac{K_S J_0}{2} t + 1\right)^2}$	$J = \frac{1}{K_i t + \frac{1}{J_0}}$	$J = \frac{J_0}{(1 + 2K_C J_0^2 t)^{\frac{1}{2}}}$

**Table 3.** Calculated mathematical parameters for the three membranes

	BW30LE4040	NF270	NF90
Complete Blocking model	$K_B=0.000313$ $R^2 = 0.95$	$K_B=0.00011$ $R^2 = 0.95$	$K_B=0.00026$ $R^2 = 0.96$
Standard Blocking model	$K_S=16.26$ $R^2 = 0.92$	$K_S=3.29$ $R^2 = 0.92$	$K_S=10.49$ $R^2 = 0.93$
Intermediate Blocking model	$K_i=17.94$ $R^2 = 0.91$	$K_i=3.29$ $R^2 = 0.91$	$K_i=11.80$ $R^2 = 0.90$
Cake Formation model	$K_C=1025196.70$ $R^2 =0.90$	$K_C=111467.48$ $R^2 =0.90$	$K_C=524237.33$ $R^2 =0.90$

**Table 4.** Results of the statistical analysis for the Complete Blocking Model

Membrane	RMSE (%)	NRMSE(-)	NSE (-)
NF270	0.025	0.031	0.95
NF90	0.029	0.041	0.97
BW30LE40	0.027	0.059	0.98

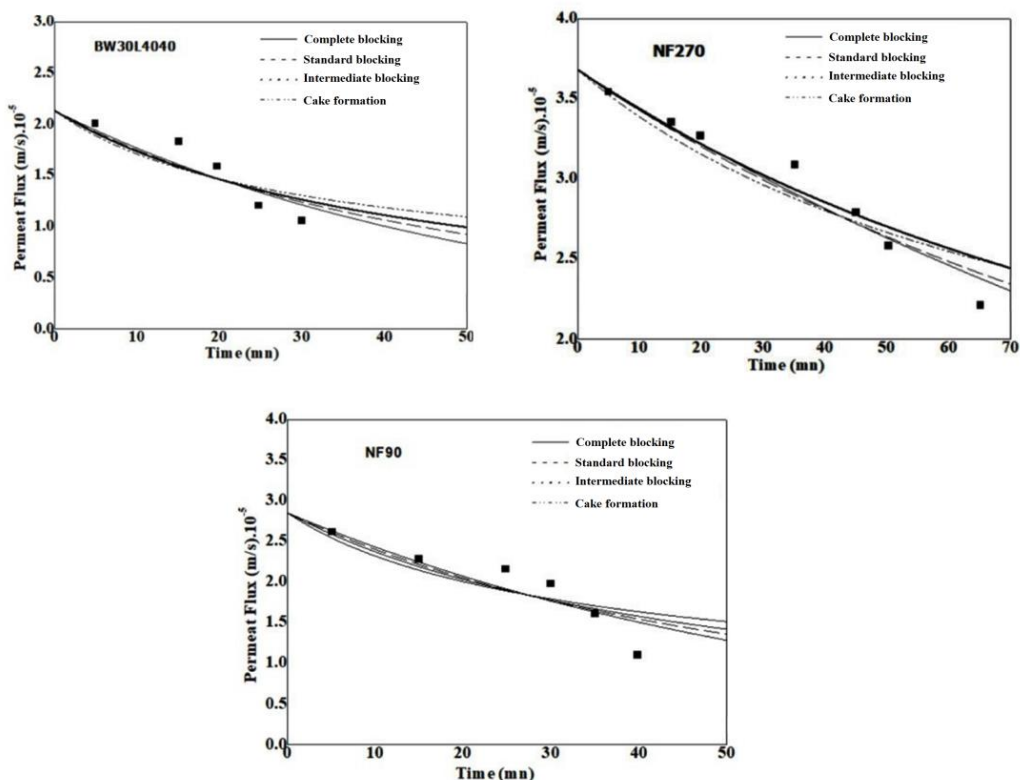


Figure 3. Permeate flux decline versus time for BW30L4040, NF270 and NF270.

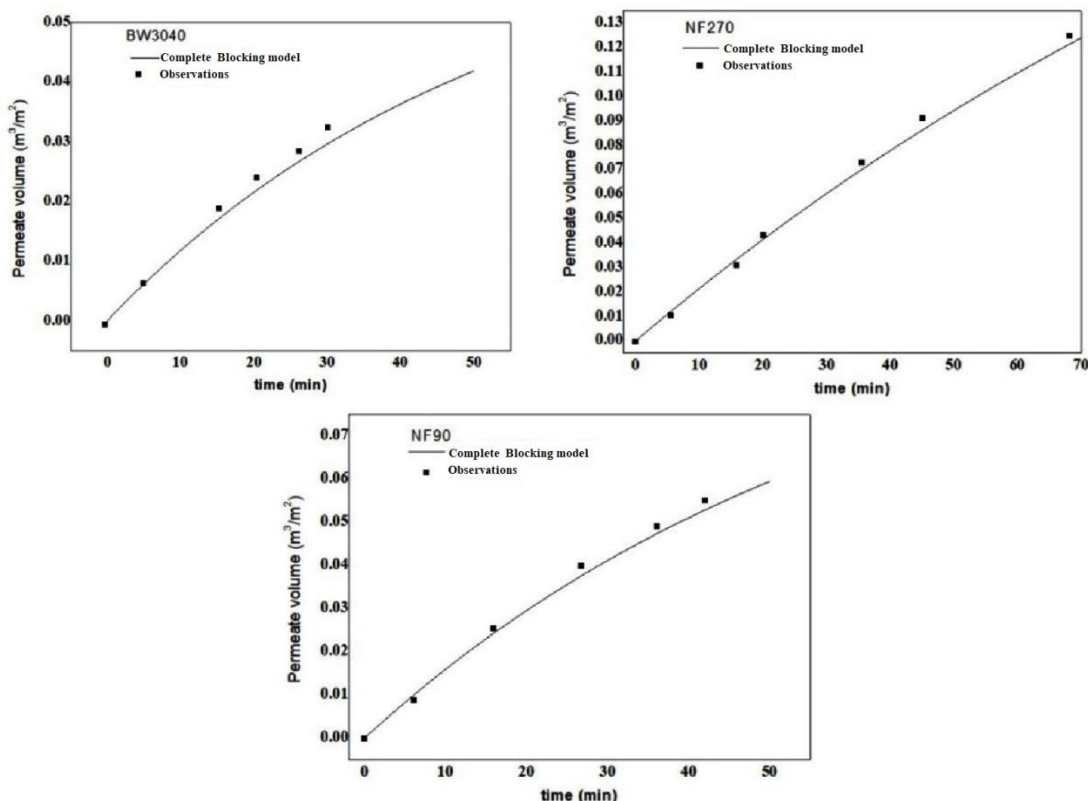


Figure 4. Cumulative permeate volume per unit membrane surface versus time for BW3040, NF270 and NF90.

CONCLUSION

In this paper, four models were applied to describe the flux decline with time in NF and RO

membranes due to fouling phenomena during desalination process: Complete Blocking Model, Standard Blocking Model, Intermediate Blocking

Model and Cake Formation Model. Results show that the Complete Blocking Model was the best representation of pore blocking for NF and RO membranes.

The given data are certainly not sufficient to verify the distinct influence of each of the proposed phenomena. This would require custom designed, more demanding experiments. Still, the example shows that the resulting model is capable of predicting the filtration decline.

#### REFERENCES

1. A. Shokri, *Bulg. Chem. Commun.*, **50**, 21 (2018).
2. A. Shokri, *Bulg. Chem. Commun.*, **50**, 27 (2018).
3. A. Shokri, M. N. Shoja, *Bulg. Chem. Commun.*, **50**, 1 (2018).
4. A. Shokri, *Iran. J. Chem. Chem. Eng.*, **38**, 5 (2019).
5. M. Bchiti, M. Igouzal, F. El Azhar, H. Oudda, A. El Midaoui, *Bulg. Chem. Commun.*, **51**, 625 (2019).
6. N. Zouhri, M. Igouzal, M. Larif, M. Hafsi, M. Taky, A. Elmidaoui, *Desal. Water Treat.*, **120**, 41 (2018).
7. M. Igouzal, F. El Azhar, M. Hafsi, M. Taky, A. Elmidaoui, *Desal. Water Treat.*, **93**, 30 (2017).
8. E. Iritani, *Drying Tech.*, **31**, 146 (2013).
9. G. L. Salinas-Rodriguez Amy, J. C. Schippers, M. D. Kennedy, *Desalination*, **365**, 79 (2015).
10. E. Iritani, S. Tachi, T. Murase, *Colloid Surface A*, **89**, 15 (1994).
11. V. L. Vilker, *AIChE Journal*, **27**, 632 (1981).
12. J. Hermia, *Trans. Inst. Chem. Eng.* **60**, 183 (1982).
13. S. El-Ghzizel, H. Zeggar, M. Tahaikt, F. Tiyal, A. Elmidaoui, M. Taky, *J. WaterProcess. Eng.*, **36**, 1 (2020).
14. El-Ghzizel, H. Jalte, H. Zeggar, M. Zait, S. Belhamidi, F. Tiyal, M. Hafsi, M. Taky, A. Elmidaoui, *Membr. Water Treat.*, **10**, 277 (2019).
15. W. R. Bowen, J. I. Calvo, A., Hernández, *J. Membrane Sci.*, **101**, 153 (1995).
16. C. Rai, P. Rai, G. C. Majumdar, S. De, S. DasGupta, *Food Bioprocess Tech.*, **3**, 545(2010).
17. S. T. D. Barros, C. M. G Andrade, E. S. Mendes, L. Peres, *J. Membrane Sci.*, **215**, 213 (2003).